Metallomics

Accepted Manuscript

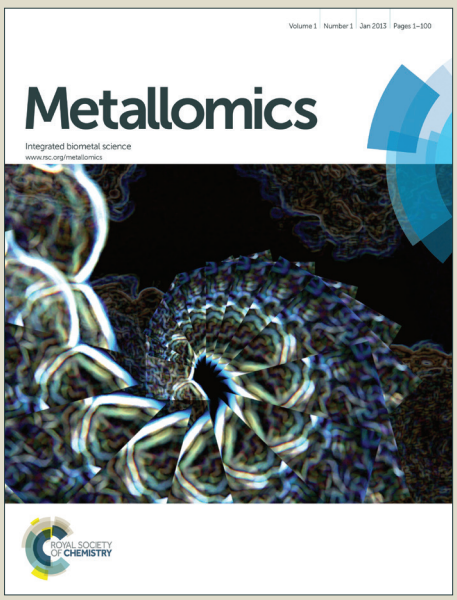

ROYAL SOCIETY OF CHEMISTRY

www.rsc.org/metallomics

Table of Content

We discuss the development and application of genetically-encoded FRET sensors as attractive tools to study intracellular Zn^{2+} homeostasis and signaling.

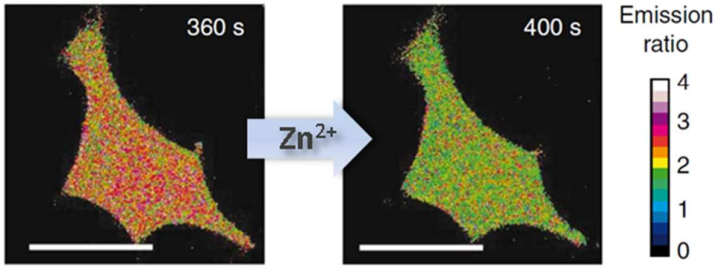

Journal Name RSCPublishing

ARTICLE

Genetically-encoded FRET-based sensors for monitoring Zn^{2+} in living cells

Cite this: DOI: 10.1039/x0xx00000x

Received 00th January 2012,
Accepted 00th January 2012

DOI: 10.1039/x0xx00000x

www.rsc.org/

Anne M. Hessels and Maarten Merkx

Abstract. Genetically-encoded fluorescent sensor proteins are attractive tools for studying intracellular Zn^{2+} homeostasis and signaling. Here we provide an overview of recently developed sensors based on Förster Resonance Energy Transfer (FRET). The pros and cons of the various sensors are discussed with respect to Zn^{2+} affinity, dynamic range, intracellular targeting and multicolor imaging. Recent applications of these sensors are described, as well as some of the challenges that remain to be addressed in future research.

Laboratory of Chemical Biology and Institute of Complex Molecular Systems, Department of Biomedical Engineering, Eindhoven University of Technology, Eindhoven, The Netherlands

1. Introduction

Transition metal ions such as iron, copper and zinc pose an interesting dilemma for all living organisms. Their unique chemical properties make them essential cofactors in numerous enzymes and proteins, which is reflected by their relatively high intracellular concentration of 10-100 μM [1]. At the same time, transition metal ions are known to be highly toxic in their free form. For iron and copper this toxicity is mainly associated with their redox activity, which renders them potent catalysts to generate free radical species. The toxicity of free Zn^{2+} is due to its high affinity for a variety of amino acid site chains such as histidines, cysteines, and to a lesser extend aspertates and glutamates, which allows Zn^{2+} to bind to numerous proteins even at nanomolar concentrations, resulting in enzyme inhibition or induction of protein-protein interactions. The mechanisms that cells have developed to control this delicate balance depend on the type of metal ion and may differ between organisms. In eukaryotes specific copper chaperone proteins transfer Cu^{+} to various cellular targets without releasing it into the cytosol [2], making Cu^{+} transport kinetically controlled. In contrast, intracellular Zn^{2+} homeostasis is believed to be thermodynamically controlled by buffering the intracellular free Zn^{2+} concentration at a level that is sufficient to supply Zn^{2+} to native Zn-proteins, but below that of toxic levels.[3, 4]. Whereas the free Zn^{2+} concentration in the cytosol is now known to be 0.1-1 nM, the free Zn^{2+} concentration in subcellular organelles is less well-established but is likely to differ substantially. For example, mM concentrations of total Zn^{2+} have been reported for pancreatic β cell granules [5] and inferred for secretory vesicles in neuronal [6] and mast cells [7], and release of Zn^{2+} from some of these organelles has been implicated to allow Zn^{2+} to act as a second messenger molecule in which transient changes in cytosolic free Zn^{2+} regulate enzymes such as protein phosphatases and caspases [8-13].

To provide a more detailed understanding of the regulation of zinc homeostasis and the role of Zn^{2+} in (intracellular) signal transduction, tools are required that allow (sub)cellular imaging of Zn^{2+} concentrations in single living cells in real time. Fluorescence is ideally suited for this purpose, because it combines high sensitivity with subcellular resolution and is not invasive [14-16]. In order to be useful, fluorescent sensors should have an appropriate affinity for Zn^{2+} under physiological conditions, show high selectivity for zinc over other bioavailable metals and translate Zn^{2+}- binding into a strong increase in fluorescence, or even better, a change in emission and/or excitation ratio. Following the development of Zinquin as the first Zn^{2+}-specific fluorescent sensor 20 years ago, the development of small molecule fluorescent sensors has been an active area in chemical biology, yielding an impressive variety of Zn^{2+} sensitive fluorescent dyes[8, 17, 18]. While synthetic probes are still the most commonly used probes for intracellular Zn^{2+} imaging, they have some important limitations such as a lack of control over subcellular localization and concentration[19].

Genetically encoded fluorescent sensors offer several advantages compared to small-molecule based probes. Protein-based probes are produced by the cell itself, which in principle allows control over their concentration, prevents leakage, and provides control over intracellular localization. In contrast, small-molecule probes need to enter the cell via diffusion over

the cell membrane. Although they can be trapped inside the cell via hydrolysis of methylesters by intracellular esterases, controlling their concentration is challenging and sometimes results in high accumulation of the probe inside cells, which can interfere with Zn^{2+} homeostasis. In addition, it is difficult to control their subcellular localization, which is an important caveat given that Zn^{2+} concentrations can vary a lot between different organelles. Another advantage of protein-based sensors is the excellent affinity and specificity displayed by natural metal binding proteins, which can be further improved by both rational and directed evolution approaches. Finally, the use of genetically-encoded probes allows easy distribution and replication of the probes via standard molecular biology techniques, and many of the probes that are discussed here are available through depositories such as AddGene.

In this review we provide an overview of the various genetically-encoded fluorescent Zn^{2+} sensors that have recently been developed. We focus on sensors that are based on Förster Resonance Energy Transfer (FRET), as these have so far proven to be the most useful for detecting Zn^{2+} in biological samples. We will not discuss semi-synthetic systems that combine a part that is genetically-encoded (which allows for subcellular targeting) with a synthetic moiety that needs to be added externally[8]. The pros and cons of the various sensors are discussed with respect to Zn^{2+} affinity and specificity, pH sensitivity, dynamic range, intracellular targeting and multicolor imaging. Finally we identify some of the challenges that remain for future research.

2. Genetically encoded FRET-based Zn2+ sensors

Several examples have been reported of Zn^{2+}-sensors consisting of a single fluorescent domain. However, most of these sensors suffer from a relatively low Zn^{2+} affinity and are intensity-based, which means that their fluorescence intensity increases or decreases upon Zn^{2+} binding without affecting their spectral properties.[20] For quantitative intracellular applications this is a disadvantage, because the fluorescent signal will not only depend on the Zn^{2+} concentration but also be affected by the absolute sensor concentration and background fluorescence. A more robust strategy to design fluorescent sensor proteins is to take advantage of Förster Resonance Energy Transfer (FRET) between two fluorescent domains. FRET is a phenomenon in which excitation energy is transferred from a donor to an acceptor fluorescent domain. Because the efficiency of energy transfer is dependent on the distance and orientation between the fluorophores, FRET is an excellent mechanism to detect conformational changes that result from metal binding to a receptor domain. Most FRET sensors use cyan fluorescent protein (CFP) and yellow fluorescent protein (YFP) as a FRET pair, but recently several sensors containing red shifted FRET pairs have been reported[21, 22]. An important property of FRET-based sensors is that the ratio of acceptor to donor emission provides information on the number of unoccupied and occupied metal sensor binding sites. This ratio is dependent on the Zn^{2+} concentration and the affinity of the sensor, but independent of the sensor concentration. FRET sensors are thus by definition ratiometric. By convention the acceptor over donor emission is used throughout this review and in most of the literature. Because metal binding and fluorescence are confined to separate domains, the design of a FRET sensor is in principle modular and new FRET sensor can be obtained by simply exchanging the metal binding or the fluorescent domains. Developing FRET sensors with a large change in emission ratio can be challenging, however, and often requires a lot of optimization. Other important sensor properties that determine the suitability of FRET-based sensors for intracellular Zn^{2+} imaging are their Zn^{2+} affinity and specificity, their binding kinetics, and their pH sensitivity. In this next paragraph we discuss the various FRET-based Zn^{2+} sensor systems that have been developed thus far.

2.1 CALWY sensors

The CALWY sensors consist of two small metal binding domains, ATOX1 and WD4, that each contain a metal binding CXXC motif, fused by a long and flexible linker. The two metal binding domains are flanked by donor and acceptor fluorescent domains, which in the initial sensor were ECFP and EYFP (CFP-Atox1-Linker-WD4-YFP, hence CALWY) (Figure 1A)[17, 23]. ATOX 1 and WD4 are Cu(I) binding domains that are involved copper homeostasis, as the sensor was initially developed to create a genetically encoded Cu^{+} sensor based on the Cu^{+}-induced dimerization of these two domains. Unexpectedly, binding of Zn^{2+} to the 4 cysteines in ATOX1 and WD4 was found to form a very stable tetrahedral complex, yielding a K_d ~0.2 pM at pH 7.1. This first CALWY sensor showed only a modest, 15% decrease in emission ratio upon Zn^{2+} binding, however. Subsequently, a series of so-called eCALWY sensors were developed with a 6-fold larger change in emission ratio and a broad range of Zn^{2+} affinities. The original ECFP and EYFP domains were substituted by Cerulean and Citrine, respectively, to increase the intensity of the donor (Cerulean) and the pH stability of the acceptor (Citrine). Two mutations (S208F and V224L) were introduced on both Cerulean and Citrine to promote intramolecular complex formation between the two fluorescent domains in the absence of Zn^{2+}. This intramolecular interaction is disrupted upon binding of Zn^{2+} to ATOX1 and WD4, which results in 2-fold decrease in emission ratio. Although the interaction between the fluorescent domains competes with Zn^{2+} binding, the overall K_d for Zn^{2+} binding of eCALWY-1 remained very high, with a K_d of 2 pM at pH 7.1 (Figure 1B)[24].

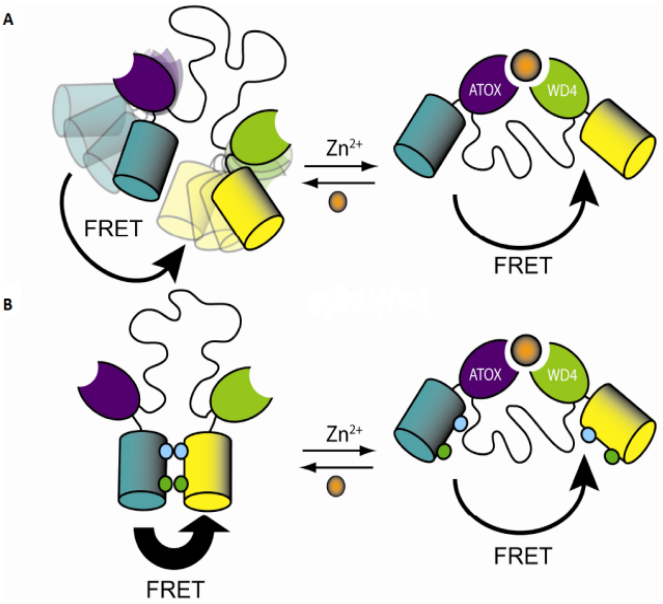

Figure 1: Scheme showing the difference between the CALWY (A) and eCALWY-1 (B) sensors. Both sensors contain two metal binding domains, ATOX1 and WD4, that are connected via a flexible peptide linker and flanked by cyan and yellow fluorescent domains. (A) In the CALWY sensor the average amount of FRET in the Zn^{2+}-free state is only slightly higher than that in the Zn^{2+}-bound state. (B) In eCALWY the FRET in the Zn^{2+}-free state is enhanced by promoting an intramolecular interaction between the fluorescent domains. Disruption of this interaction upon Zn^{2+} binding results in a large decrease in FRET. Adapted from reference [24].

eCALWY-1 was initially tested in both HEK293 cells and INS-1(832/13) cells. The ratio of Citrine over Cerulean emission was measured for individual cells following excitation of Cerulean (Figure 2A). An increase in emission ratio was observed after addition of TPEN, a very high affinity cell-permeable Zn^{2+} chelator, which is consistent with dissociation of Zn^{2+} from the sensor. As expected, subsequent addition of excess Zn^{2+} in the presence of the ionophore pyrithione resulted in a decrease in emission ratio. Since the ratio at the start of the experiment was the same as in the presence of excess Zn^{2+}, the eCALWY-1 sensor was already fully occupied with Zn^{2+}, suggesting that the Zn^{2+} affinity of eCALWY-1 was actually too high to reliably measure the cytosolic free Zn^{2+} concentration. Therefore the Zn^{2+} affinity of eCALWY-1 was systematically attenuated, creating a toolbox of eCALWY-based sensor ranging in affinity between 2 pM and 3 nM at physiological pH. Introduction of a single cysteine-to-serine mutation in the Zn^{2+} binding pocket of the sensor yielded eCALWY-4, which has a 300-fold weaker affinity for Zn^{2+} (K_d = 630 pM). This mutation also abrogated Cu^{+} binding to the protein, as eCALWY-4 did not show any response up to micromolar Cu^{+} levels. Further fine tuning of the Zn^{2+} affinity was achieved by shortening the flexible peptide linker between the metal binding domains from 9 GGSGGS repeats in eCALWY-1 and ecALWY-4 to 5 GGSGGS repeats (eCALWY2, and eCALAY-5) and 3 GGSGGS repeats (eCALWY-3 and eCALWY-6; Table 1).

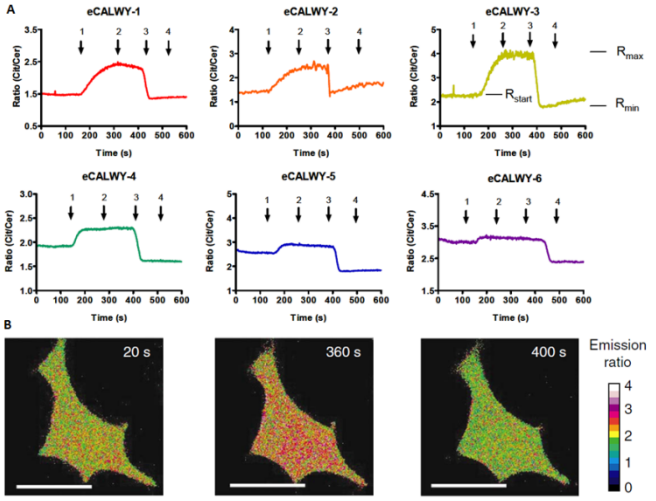

Figure 2: (A) Responses of single INS-1(832/13) cells expressing different eCALWY variants to subsequent addition of 50 µM TPEN (1) 5 µM pyrithione (2), 5 µM pyrithione/100 µM Zn^{2+} (3) and buffer (4). Each traces shows the response of an representative individual cell. The emission ratios R_{start}, R_{max}, and R_{min} can be used to calculate the sensor occupancy. (B) False-color spinning disc confocal microscopy images of INS-1(832/13) cells expressing eCALWY-4 after perfusion with buffer (20 s), buffer with 50 µM TPEN (360 s), and buffer with 5 µM pyrithione/100 µM Zn^{2+} (400 s). Scale bar, 15 µm. Adapted from reference [24].

Figure 2 shows the responses of INS-1(832/13) cells transiently expressing one of the six eCALWY variants to the addition of TPEN and the subsequent treatment with Zn^{2+} and pyrithione. For all sensors the in situ response was consistent with the in vitro determined Zn^{2+} affinity, with the high affinity eCALWY-1 being fully saturated, while the sensor with the lowest affinity (eCALWY-6) being nearly empty at the start of the experiment.

$$occupancy = (R_{max}-R_{start})/(R_{max}- R_{min})\cdot 100\% \qquad (1)$$

Equation 1 can be used to estimate the Zn^{2+} occupancy under steady state conditions. R_{max} and R_{min} are the emission ratios after TPEN and pyrithione/Zn^{2+} addition, respectively, and R_{start} is the ratio at the start of the experiment (Figure 2). This procedure is necessary because the emission ratio observed for cells expressing the same sensor may vary substantially between cells, e.g. because of varying contributions of background fluorescence. Although calibration by determining R_{max} and R_{min} provides at present the best method to estimate the sensor occupancy (and from that the free Zn^{2+} concentration), it has recently been shown that assuming a linear relationship between relative emission ratio and sensor occupancy is not always valid[25]. Some care should therefore be taken to not over interpret the accuracy with which the free Zn^{2+} concentration can be determined, especially when the determination is based on the response of a single sensor. This is particularly true when the sensor's affinity is not close to the free Zn^{2+} concentration. In the case of the eCALWY sensors, determination of the free Zn^{2+} concentration using eCALWY-4 is therefore more reliable than using e.g. eCALWY-2. A final assumption in the calculation of the free Zn^{2+} concentration is that the sensor's K_d, which is most accurately determined in

vitro, is not significantly affected by intracellular conditions such as increased ionic strength and macromolecular crowding. For eCALWY-4 this was shown to be true at least in the cytosol, where in-situ calibration with the pore-forming protein α-toxin and a Zn^{2+} buffer solution showed that the apparent K_d was only slightly lower in situ than obtained in vitro using purified sensor protein.

Table 1: Overview of different FRET-based Zn^{2+} sensors

Sensor variant	Ratiometric change (in vitro)	K_d (pH 7.1)		ref.
CALWY (Cys_4)	15%	0.2	pM	17
eCALWY-1 (Cys_4)	240%	2	pM	24
eCALWY-2 (Cys_4)	270%	9	pM	24
eCALWY-3(Cys_4)	215%	45	pM	24
eCALWY-4 (Cys_3)	250%	630	pM	24
eCALWY-5 (Cys_3)	300%	1850	pM	24
eCALWY-6 (Cys_3)	200%	2900	pM	24
		0.5	μM (pH 6.0)	
redCALWY-1 (Cys_4)	62%	12.3	pM	21
redCALWY-4 (Cys_3)	30%	234	pM	21
ZifCY1(Cys_2His_2)	220%	1.7	μM	26
ZifCY2 (His_4)	400%.	160	μM	26
ZapCY1(Cys_4)	130%	2.5	pM	27
ZapCY2(Cys_2His_2)	70%	811	pM	27
ZapOC2 (Cys_2His_2)	12%[a]	n.d.		22
ZapCmR2 (Cys_2His_2)	39%[a]	n.d.		22
ZapCmR1 (Cys_4)	16%[a]	n.d.		22
ZinCh-9 (Cys_2)	360%	213	nM (pH 8.0)	28
eZinCh-1 (Cys_2)	800%	8.2 253 250	μM nM (pH8.0) μM (pH 6.0)	24
CLY9-2His (2 His_6-tags)	65%	47	nM (pH 8.0)	29

[a] ratiometric change was determined in situ

In general, the reliability of determining the free Zn^{2+} concentration can be increased by performing measurements with sensors with different affinities. For example, plotting the sensor occupancies for all six eCALWY variants as a function of their K_d revealed that their responses were all consistent with a free Zn^{2+} concentration ~ 0.4 nM, both in mouse pancreatic beta cells INS-1(832/13) and in HEK293 cells. Subsequent work in other cell types and using these and other sensors (see below) confirmed that the cytosolic Zn^{2+} in mammalian cells is relatively well-buffered between 100 pM and 1 nM. Because genetically encoded fluorescent proteins are constitutively expressed they have become part of the cellular Zn^{2+} buffer machinery, which explains why, unlike synthetic fluorescent Zn^{2+} sensors, there occupancy does not depend on their absolute concentration and why their presence at μM concentrations does not seem to perturb the cytosolic free Zn^{2+} concentration[30].

Although most studies using genetically encoded FRET sensors such as eCALWY have been done in cell lines using transient transfection, FRET sensors have also been used in primary cells such as pancreatic β-cells, neurons[31] and cardiomyocytes (Chabosseau et. al., submitted). To allow transfection of primary cells, the Rutter lab cloned several eCALWY variants into an adenovirus system[32]. Using primary islet cells infected with eCALWY-4-expressing adenovirus, treatment with high glucose levels was found to result in a 2-fold increase in cytosolic Zn^{2+} concentrations. Another recent application of the eCALWY sensors was reported by the Frommer group, who used these sensors to image cytosolic Zn^{2+} concentrations in the root tips of *Arabidopsis thalania*. An *Arabidopsis thalania* line that is deficient in transgene-induced silencing (rgr6) was used to constitutively express different cytosolic eCALWY variant[33]. Expression of the eCALWY sensors in these cell lines showed high fluorescence and did not seem to affect the viability of the expressing *Arabidopsis* lines. Imaging in root cells using the RootChip technology showed cytosolic free Zn^{2+} concentration that were similar to those found in mammalian cells. The sensors were also used to monitor the response of cytosolic free Zn^{2+} levels to the external Zn^{2+} concentrations, revealing the presence of both high and low affinity uptake systems.

One of the advantages of genetically encoded sensors compared to synthetic fluorescent probes, is that they can be targeted to specific subcellular locations by attachment of specific targeting sequences. Establishing the free Zn^{2+} concentrations in specific organelles has proven to be more challenging than in the cytosol, however, and conflicting results have been obtained using different genetically encoded sensors. Both the free Zn^{2+} concentration itself and environmental parameters such as pH, redox potential, and Zn^{2+} buffer capacity may all be different in an organelle from the cytosol, making estimation of the free Zn^{2+} concentration based on the in vitro determined K_d and in situ observed sensor occupancy more uncertain. In addition, in situ calibration of the sensors is also more challenging as 2 or more cellular membranes need to be crossed. Recent work by Chabosseau found that ER-targeted eCALWY-4 was almost completely saturated with Zn^{2+} in a variety of cell lines and primary cardiomyocytes, suggesting that the free Zn^{2+} concentration in the ER is higher than in the cytosol[34]. These numbers would be consistent with a putative role for the ER as a store of Zn^{2+} from which Zn^{2+} release to the cytosol can be triggered. However, different results were previously reported by Palmer and coworkers, who, using different a FRET sensor (see below), reported free Zn^{2+} concentrations of less than 1 pM in the ER[27]. A similar discrepancy was observed for the mitochondria[31, 34]. Measurements using eCALWY-4 targeted to the mitochondrial matrix of several cell lines and primary cells, consistently yielded free Zn^{2+} concentrations of 200-300 pM. It should be noted that these numbers were calculated based on the dissociation constant of eCALWY-4 determined at pH 7.8, which is 60 pM. Again these numbers are 3 orders of magnitude higher than were determined by the Palmer group

using the FRET sensors ZapCY1 and a semi-synthetic carbonic anhydrase-based sensor from the Thompson group, both of which have reported values of 0.2 pM[31, 35]. However, a substantially higher concentration of 72 pM was recently determined using a small molecule ratiometric fluorescent probe targeted to the mitochondria of NIH 3T3 cells [36, 37].

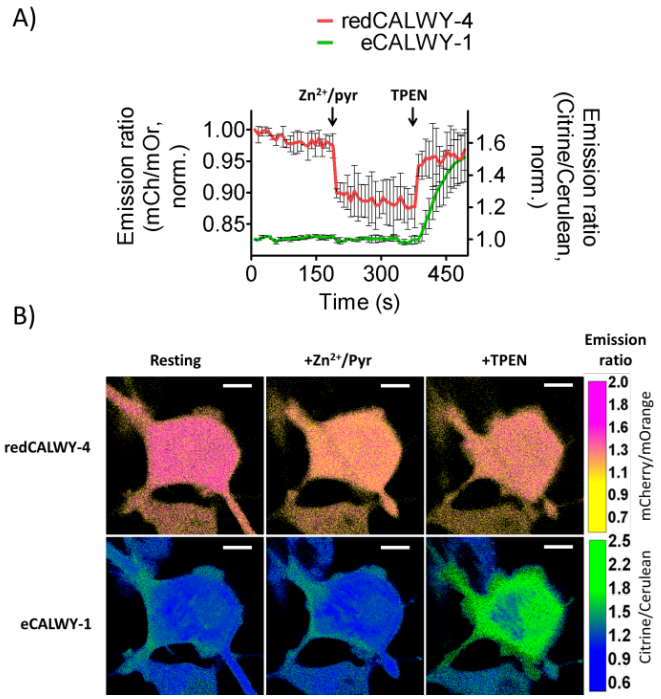

Figure 3: Simultaneous imaging of two differently colored Zn2+ FRET sensors to image Zn^{2+} over a broad concentration range in the same cellular compartment. (A) Response of HeLa cells expressing both the high-affinity eCALWY-1 (green) and moderate affinity redCALWY-4 (red) to the addition of Zn^{2+}/pyrithione followed by excess TPEN. Normalized emission ratio's averaged over multiple cells are shown. (B) False-colored ratiometric images of a representative cell in the resting state, at high Zn^{2+} concentration (+Zn^{2+}/pyr) and at low Zn^{2+} concentration (+TPEN). Adapted from reference [21].

In order to simultaneously monitor Zn^{2+} in different cellular compartments in the same cell or study the relation between Zn^{2+} concentration and intracellular signal transduction, sensor variants are required that can be used together with CFP-YFP based sensors[21]. Recently red-shifted variants of eCALWY were obtained by replacing Cerulean and Citrine by mOrange and mCherry, respectively. To obtain sensors with a sufficient FRET response, hydrophobic mutations needed to be introduced at the surface of both fluorescent domains to promote association of mOrange and mCherry in the Zn^{2+}-free state. The affinities of these redCALWY's were similar to those of the original CFP/YFP-based sensors, with K_d values of 12.3 ± 2 pM and 234 ± 5 pM for redCALWY-1 and redCALWY-4, respectively (Table 1). *In situ*, the high affinity redCALWY-1 was completely saturated with Zn^{2+} under normal physiological conditions, while the lower affinity redCALWY-4 was found to be mostly empty when expressed in the cytosol of HeLa cells. Importantly, simultaneous imaging of two spectrally distinct eCALWY variants (eCALWY-1 and redCALWY-4) in the cytosol of a single cell was successfully demonstrated (Figure 3). This experiment not only allowed measurement of cytosolic Zn^{2+} concentrations over an extended concentration range, but also shows the feasibility of monitoring Zn^{2+} concentrations at different subcellular localizations that can otherwise not be easily distinguished, such as the ER and the cytosol.

2.2 Sensors based on zinc fingers: Zif- and Zap-based FRET sensors

Zinc fingers (ZF) represent an attractive class of Zn^{2+} binding domains for the development of FRET sensors, because metal-dependent protein folding ensures a large conformational change upon Zn^{2+} binding. The Palmer group used several zinc finger domains to construct FRET sensors, resulting in sensors with a range of affinities. One of the first designs was based on the mammalian transcription factor Zif268, a ZF domain containing a Cys_2His_2 binding pocket. Two sensors were constructed by fusion of CFP and YFP at the N- and C-termini of ZF domain, one containing the wild-type zinc finger domain (ZifCY1) and one in which the cysteines were mutated to histidines (ZifCY2)[26]. In vitro, both sensors showed a large increase in emission ratio (2.2-fold and 4.0-fold, respectively) but relatively weak Zn^{2+} affinities of 1.7 µM for ZifCY1 and ~ 160 µM for ZifCY2, whereas the Zn^{2+} affinity of the Zif268 domain itself was in the low nanomolar range. In situ, the dynamic range of ZifCY1 was found be attenuated to 25%, possibly as a result of molecular crowding. Using the ZifCY1 sensor, the free cytosolic Zn^{2+} concentrations was initially estimated to be approximately 180 nM, but this number actually reflects the lower limit of detection for this sensor and the cytosolic free Zn^{2+} concentration was subsequently shown to be 1000-fold lower. This example illustrates the difficulty of measuring analyte concentrations that are outside the affinity range of a sensor, and explains the observation that higher sensor concentrations resulted in an apparent increase in the estimated intracellular Zn^{2+} level.

To obtain FRET sensors with increased Zn^{2+} affinity and improved (in-situ) dynamic range, Palmer and coworkers subsequently developed the Zap-series of FRET sensors [27]. These sensors contain the first and second zinc finger domains of the *Saccharomyces cerevisiae* transcriptional regulator Zap1, which have a low nanomolar affinity for Zn^{2+} (Figure 4). Zap1-based FRET sensors were first reported by Eide and coworkers[38], who did not use them to measure free Zn^{2+} concentrations, but to study the kinetics of Zn^{2+} binding and release in situ in yeast. Palmer and coworkers improved these sensors by linker optimization and by replacing the original CFP by a truncated variant and EYFP by the pH stable Citrine. *In vitro* characterization of the ZapCY1 sensor yielded a K_d of 2.5 pM at pH 7.4. A variant (ZapCY2) was also constructed by replacing two of the cysteines in the Zn^{2+} binding pocket by histidines, which decreased the affinity for Zn^{2+} to a K_d of 811 pM. Expression of ZapCY1 in mammalian cells showed a 4-fold decrease in emission ratio upon treatment with a zinc

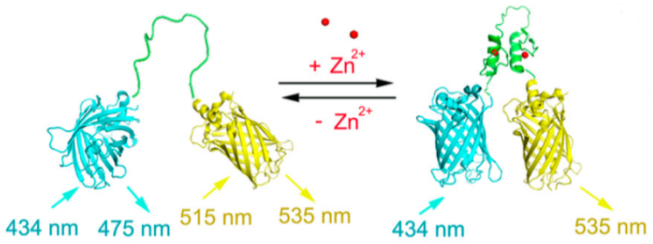

Figure 4: The high-affinity Zn^{2+} sensor ZapCY1 consists of the first and second zinc finger domains of *Saccharomyces cerevisiae* Zap1 flanked by truncated CFP and Citrine. Zn^{2+} binding induces folding of the ZF domans, resulting in an increase in FRET. Adapted from reference [27].

chelating reagent, which was completely reversed upon treatment of the cells with digitonin and excess Zn^{2+}. The complete saturation of ZapCY1 under normal physiological conditions is consistent with its high Zn^{2+} affinity, which is similar to that of eCAWLY-1 (Figure 5A). In contrast, the cytosolic ZapCY2 sensor showed a 1.4-fold change in emission ratio and was only partially occupied at the start of the experiment (Figure 5B). Based on the response of ZapCY2, a free Zn^{2+} concentration of ~80 pM was calculated, which is comparable to the previously determined concentrations using the eCALWY series[24]. Another difference between ZapCY1 and ZapCY2 is their response kinetics. Reaching the Zn-free state of ZapCY-1 in situ requires incubation with TPEN for ~30 minutes, whereas the response of ZapCY-2 occurs is much faster, making this the preferred Zap-based sensor for measuring cytosolic Zn^{2+} concentrations. The slow response of ZAPCY1 upon TPEN addition might be partially due to its tight Zn^{2+} binding, since eCALWY-1 also showed a slower response compared to the lower affinity eCALWY-4 sensor. However, despite their similar affinities for Zn^{2+}, the Zn-free state of eCALWY-1 is reached at least 5-fold faster than ZapCY-1.

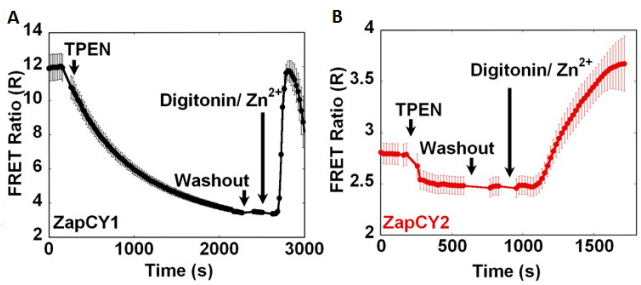

Figure 5: FRET responses of ZapCY1 (A) and ZapCY2 (B) expressed in the cytosol of HeLa cells to the addition of TPEN, followed by the addition of excess Zn^{2+} in the presence of digitonin. Adapted from reference[27].

ZapCY-1 and other ZF-based FRET sensors have been successfully targeted to a variety of organelles, including the ER, Golgi and mitochondrial matrix[27, 31]. HeLa cells expressing ZapCY1 in the ER showed a small decrease in emission ratio upon prolonged incubation with TPEN, followed by a much larger increase in emission ratio upon subsequent addition of excess Zn^{2+}. This response suggests that despite its high affinity (K_d = 2.5 pM) ZapCY1 was mostly Zn^{2+} free in the ER, and a free Zn^{2+} concentration of 0.9 pM was obtained from application of equation 1. A very similar response was observed for Golgi-targeted ZapCY1, yielding a similarly low free Zn^{2+} concentration of 0.6 pM[27]. As expected, the low affinity ZifCY1 sensor (K_d ~1.7 µM) targeted to the ER did not show any response upon addition of TPEN, indicating a Zn-free state of the sensor in the ER lumen. These data suggest that the free Zn^{2+} concentration in the ER and Golgi is maintained at a much lower concentration than in the cytosol, but it is unclear how this concentration gradient would be maintained. As discussed before, these data are strikingly different from the results obtained with the eCALWY-4, which, despite a much higher K_d, was found by be mostly saturated.

A similar discrepancy between the ZapCY1 and eCALWY sensors was observed in the mitochondrial matrix. ZAPCY-1 was targeted to the mitochondrial matrix by attachment of an N-terminal targeting sequence from human cytochrome c oxidase subunit 8a. The response of ZapCY1 targeted to the mitochondria in HeLa cells to the addition TPEN and Zn^{2+} was very similar to that observed for ER- and Golgi-targeted ZAPCY1. TPEN addition resulted in a small and slow decrease in emission ratio, whereas excess Zn^{2+} caused a fast and large increase in emission ratio. The affinity of ZAPCY1 was first corrected for the mitochondrial pH (pH 8.0), and then free mitochondrial Zn^{2+} concentration was estimated to be 0.22 pM[31]. This value is similar to that obtained using a carbonic anhydrase-based FRET sensor, but 2-3 orders of magnitude lower than those obtained using mitochondrial targeted small molecule probes and mitochondrial targeted eCALWY4. At present it is unclear why the ZapCY1 and eCALWY probes behave so different when targeted to the ER and mitochondrial matrix. It seems unlikely that this discrepancy is due to an error in the determination of Zn^{2+} affinity, because both sensors give more similar results when used in the cytosol. One way to resolve these discrepancies might be to use FRET sensors that use alternative binding mechanisms. Both sensors depend on cysteines for Zn^{2+} binding, which in the oxidizing environment of the ER lumen may cause problems with improper folding or cysteine oxidation.

Red-shifted variants have also been developed for the Zap-based FRET sensors[22]. The original CFP and YFP domains in ZapCY1 and ZapCY2 were replaced by a variety of red-shifted fluorescent domains. Their performance was assessed in both the cytosol and nucleus of HeLa cells, by *in situ* calibrations with TPEN and excess Zn^{2+}. The variant with the largest change in emission ratio (~40%) consisted of the green fluorescent donor Clover and mRuby2 as a red fluorescent acceptor. Spectral overlap between CFP-YFP and Clover/mRuby2 makes simultaneous imaging in the same cellular compartment challenging with these sensors, but simultaneous intracellular imaging was achieved by targeting the Clover/mRuby2-based sensor to the nucleus. Sensor variants with orange and red fluorescent domains, which are spectrally well separated from CFP and YFP, were also obtained but unfortunately displayed relatively small changes in

emission ratio of ~10% changes. The replacement of the fluorescent domains seemed to sometimes affect the Zn^{2+} affinity, since some variation in sensor occupancy was reported between different variants that were based on the same metal binding domain.

2.3 eZinCh and His-tag based FRET sensors

High affinity Zn^{2+} sensors such as the eCALWY and ZapCY sensors are necessary for imaging free Zn^{2+} in the cytosol and organelles such as the nucleus, mitochondria and possibly the ER. However, concentrations of free Zn^{2+} can be substantially higher in secretory vesicles and in the extracellular milieu. An example are the insulin secreting vesicles in pancreatic beta cells, which store insulin in complex with Zn^{2+} and contain mM concentrations of total Zn^{2+}. eCALWY-6, which has a K_d of 0.5 µM at the vesicular pH of 6.0, was found to be fully saturated when targeted to these vesicles[24]. To reliably measure these higher concentrations of Zn^{2+}, sensors are needed that have affinities in the high nanomolar to low micromolar regime. Here we describe two examples of such moderate affinity sensors, eZinCh and His-tag based sensors.
The ZinCh sensors are fusion proteins of ECFP and EYFP connected via a long flexible peptide linker. Instead of relying on a separate Zn^{2+} binding domain, two Zn^{2+} coordinating amino acids (Y39H and S208C) were introduced directly on the so-called dimerization interface of each of the fluorescent domains (Figure 6)[28].

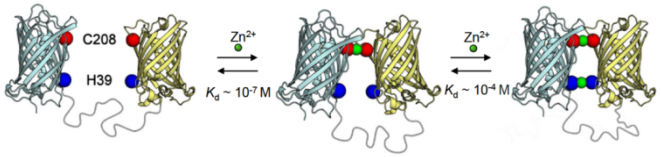

Figure 6: ZinCh-9 is a moderate affinity Zn^{2+} sensor that displays a biphasic increase in FRET upon Zn^{2+} binding. Binding of Zn^{2+} to cysteines at position 208 of ECFP and EYFP brings both domains together, which is followed by binding of Zn^{2+} to two histidines introduced at position 39. Adapted from reference[28].

Addition of Zn^{2+} resulted in a biphasic 4-fold increase in emission ratio, covering Zn^{2+} concentrations between 100 nM and 1 mM (at pH 8). The first, high affinity Zn^{2+} binding event (K_{d1} = 200 nM at pH 8.0) involves the coordination of Zn^{2+} between the two Cys208 residues, which results in formation of an intramolecular complex between ECFP and EYFP in a parallel orientation. Next, a second Zn^{2+} binds to a lower affinity site created by the two His39 residues (K_{d2} ~ 88 µM at pH 8.0), resulting in a further increase in emission ratio. Importantly, ZinCh was shown to be specific for Zn^{2+} over other divalent metal ions such as Cd^{2}, Ni^{2+}, Mg^{2}, and Ca^{2+}. An improved sensor variant (eZinCh-1) with an 8-fold increase in emission ratio was created by replacing ECFP and EYFP by cerulean and citrine and by removing the low affinity binding site. The Zn^{2+} affinity of eZinCh-1 was found to be strongly pH dependent, changing from K_d = 258 nM at pH = 8.0, to 8.2 µM at pH 7.1, and 250 µM at pH 6.0. An effort to increase the Zn^{2+} affinity by creating a tetrahedral Cys_4 binding site at the dimerization interface failed, but increased affinity was observed for Cd^{2+}, which has larger ionic radius than Zn^{2+}. These results suggest that the four cysteine binding pocket is too large to efficiently bind Zn^{2+} [39]. Recently, an eZinCh variant was developed that displays a substantially higher Zn^{2+} affinity (K_d of 1 nM at pH 7.1; Hessels et al, unpublished results).

To test the suitability of eZinCh-1 for measuring vesicular Zn^{2+}, the sensor was targeted to the secretory granules of INS-1 (832/13) cells by fusion of the sensor to vesicle-associated membrane protein 2 (VAMP2)[24]. Co-localization studies confirmed exclusive localization of the sensor in insulin containing granules. Under resting conditions low emission ratios were observed of eZinCh-1 in the vesicles, which indicates that the sensor was completely empty at the start of the experiment. Addition of extracellular Zn^{2+} and pyrithione did not change the emission ratio, suggesting that this treatment is not sufficient to raise the free Zn^{2+} concentration above the ~50 µM that would be required to allow Zn^{2+} binding at pH 6.0 (K_d 250 µM at pH 6.0; Table 1). To test whether the eZinCh-1 was indeed empty because of the low vesicular pH, cells were treated with the Na^{+}/H^{+} exchanger inhibitor monensin, which transiently increases the pH from 6.0 to 7.0. Indeed, a robust increase in emission ratio was observed upon treatment with monensin, which was fully reversible after monensin was washed out. Although the functionality of vesicular-targeted eZinCh-1 was established, these results also show that monitoring vesicular free Zn^{2+} concentrations ideally requires the development of less pH sensitive FRET sensors with a Zn^{2+} affinity of ~ 10 µM at pH 6.0.

The sensors discussed so far are all redox sensitive, as they rely at least partially on cysteines for Zn^{2+} binding. A sensor that binds Zn^{2+} exclusively using histidines was created based on the observation that Zn^{2+} forms a relatively stable 1:2 complex with His-tags[29]. This sensors consists of a fusion protein of ECFP and EYFP connected a long flexible peptide linker, with $(His)_6$ tags introduced at both the N-and C-termini (Figure 7).

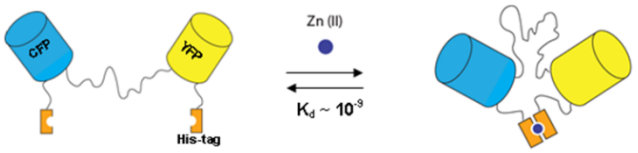

Figure 7: FRET sensor design based on His-tags as Zn^{2+} binding sites. Zn^{2+} binding to His-tags at the N-and C-termini results in the formation of a compact intramolecular Zn^{2+} complex with a moderate Zn^{2+} affinity. Adapted from reference[29].

Intramolecular binding of Zn^{2+} between the 2 His-tags brings ECFP and EFYP in close proximity, which results in a 1.6-fold increase in emission ratio and a K_d for Zn^{2+} of 50 nM at pH = 8.0. This sensor has not been applied for cellular imaging, but has recently been used to determine the concentration of free Zn^{2+} in blood serum (Arts et al, unpublished results). Future development of this sensor may involve the replacement ECFP

and EYFP by improved or differently colored fluorescent domains and the optimization of Zn^{2+} coordination by the His-tags. In addition to in vitro diagnostic applications these improved variants could also proof useful for intracellular imaging applications involving oxidizing and/or acidic conditions.

Acknowledgements

Our work on genetically-encoded fluorescent probes is supported by grants from The Netherlands Organization of Scientific Research (ECHO grant 700.59.013) and an ERC starting grant (ERC-2011-StG 280255). The authors would like to acknowledge the contribution of the Zinc-Net COST Action TD 1304.

References

1. M. Valko, H. Morris and M. T. Cronin, Metals, toxicity and oxidative stress, *Curr Med Chem*, 2005, **12**, 1161-1208.
2. T. D. Rae, P. J. Schmidt, R. A. Pufahl, V. C. Culotta and T. V. O'Halloran, Undetectable intracellular free copper: the requirement of a copper chaperone for superoxide dismutase, *Science*, 1999, **284**, 805-808.
3. R. J. Cousins, J. P. Liuzzi and L. A. Lichten, Mammalian zinc transport, trafficking, and signals, *J Biol Chem*, 2006, **281**, 24085-24089.
4. A. Krezel and W. Maret, Zinc-buffering capacity of a eukaryotic cell at physiological pZn, *J Biol Inorg Chem*, 2006, **11**, 1049-1062.
5. J. C. Hutton, E. J. Penn and M. Peshavaria, Low-molecular-weight constituents of isolated insulin-secretory granules. Bivalent cations, adenine nucleotides and inorganic phosphate, *Biochem J*, 1983, **210**, 297-305.
6. D. H. Linkous, J. M. Flinn, J. Y. Koh, A. Lanzirotti, P. M. Bertsch, B. F. Jones, L. J. Giblin and C. J. Frederickson, Evidence that the ZNT3 protein controls the total amount of elemental zinc in synaptic vesicles, *J Histochem Cytochem*, 2008, **56**, 3-6.
7. L. H. Ho, R. E. Ruffin, C. Murgia, L. Li, S. A. Krilis and P. D. Zalewski, Labile zinc and zinc transporter ZnT4 in mast cell granules: role in regulation of caspase activation and NF-kappaB translocation, *J Immunol*, 2004, **172**, 7750-7760.
8. K. P. Carter, A. M. Young and A. E. Palmer, Fluorescent sensors for measuring metal ions in living systems, *Chem. Rev.*, 2014, **114**, 4564-4601.
9. J. Kaltenberg, L. M. Plum, J. L. Ober-Blobaum, A. Honscheid, L. Rink and H. Haase, Zinc signals promote IL-2-dependent proliferation of T cells, *Eur J Immunol*, 2010, **40**, 1496-1503.
10. W. Maret, Inhibitory zinc sites in enzymes, *Biometals*, 2013, **26**, 197-204.
11. K. M. Taylor, S. Hiscox, R. I. Nicholson, C. Hogstrand and P. Kille, Protein Kinase CK2 Triggers Cytosolic Zinc Signaling Pathways by Phosphorylation of Zinc Channel ZIP7, *Sci Signal*, 2012, **5**.
12. M. Wilson, C. Hogstrand and W. Maret, Picomolar Concentrations of Free Zinc(II) Ions Regulate Receptor Protein-tyrosine Phosphatase beta Activity, *J Biol Chem*, 2012, **287**, 9322-9326.
13. S. Yamasaki, A. Hasegawa, S. Hojyo, W. Ohashi, T. Fukada, K. Nishida and T. Hirano, A Novel Role of the L-Type Calcium Channel alpha(1D) Subunit as a Gatekeeper for Intracellular Zinc Signaling: Zinc Wave, *Plos One*, 2012, **7**.
14. K. Kikuchi, Design, synthesis and biological application of chemical probes for bio-imaging, *Chem Soc Rev*, 2010, **39**, 2048-2053.
15. D. W. Domaille, E. L. Que and C. J. Chang, Synthetic fluorescent sensors for studying the cell biology of metals, *Nat Chem Biol*, 2008, **4**, 168-175.
16. K. M. Dean, Y. Qin and A. E. Palmer, Visualizing metal ions in cells: an overview of analytical techniques, approaches, and probes, *Biochim. Biophys. Acta*, 2012, **1823**, 1406-1415.
17. E. M. van Dongen, T. H. Evers, L. M. Dekkers, E. W. Meijer, L. W. Klomp and M. Merkx, Variation of linker length in ratiometric fluorescent sensor proteins allows rational tuning of Zn(II) affinity in the picomolar to femtomolar range, *J Am Chem Soc*, 2007, **129**, 3494-3495.
18. R. A. Bozym, R. B. Thompson, A. K. Stoddard and C. A. Fierke, Measuring picomolar intracellular exchangeable zinc in PC-12 cells using a ratiometric fluorescence biosensor, *ACS Chem Biol*, 2006, **1**, 103-111.
19. E. M. Nolan and S. J. Lippard, Small-molecule fluorescent sensors for investigating zinc metalloneurochemistry, *Acc Chem Res*, 2009, **42**, 193-203.
20. J. L. Vinkenborg, M. S. Koay and M. Merkx, Fluorescent imaging of transition metal homeostasis using genetically encoded sensors, *Curr Opin Chem Biol*, 2010, **14**, 231-237.
21. L. H. Lindenburg, A. M. Hessels, E. H. Ebberink, R. Arts and M. Merkx, Robust red FRET sensors using self-associating fluorescent domains, *ACS Chem Biol*, 2013, **8**, 2133-2139.
22. J. G. Miranda, A. L. Weaver, Y. Qin, J. G. Park, C. I. Stoddard, M. Z. Lin and A. E. Palmer, New alternately colored FRET sensors for simultaneous monitoring of Zn^{2+} in multiple cellular locations, *Plos One*, 2012, **7**, e49371.
23. E. M. van Dongen, L. M. Dekkers, K. Spijker, E. W. Meijer, L. W. Klomp and M. Merkx, Ratiometric fluorescent sensor proteins with subnanomolar affinity for Zn(II) based on copper chaperone domains, *J Am Chem Soc*, 2006, **128**, 10754-10762.
24. J. L. Vinkenborg, T. J. Nicolson, E. A. Bellomo, M. S. Koay, G. A. Rutter and M. Merkx, Genetically encoded FRET sensors to monitor intracellular Zn^{2+} homeostasis, *Nat Methods*, 2009, **6**, 737-740.
25. A. Pomorski, T. Kochanczyk, A. Miloch and A. Krezel, Method for accurate determination of dissociation constants of optical ratiometric systems: chemical probes, genetically encoded sensors, and interacting molecules, *Anal Chem*, 2013, **85**, 11479-11486.
26. P. J. Dittmer, J. G. Miranda, J. A. Gorski and A. E. Palmer, Genetically encoded sensors to elucidate spatial distribution of cellular zinc, *J Biol Chem*, 2009, **284**, 16289-16297.

27. Y. Qin, P. J. Dittmer, J. G. Park, K. B. Jansen and A. E. Palmer, Measuring steady-state and dynamic endoplasmic reticulum and Golgi Zn^{2+} with genetically encoded sensors, *Proc Natl Acad Sci U S A*, 2011, **108**, 7351-7356.
28. T. H. Evers, M. A. Appelhof, P. T. de Graaf-Heuvelmans, E. W. Meijer and M. Merkx, Ratiometric detection of Zn(II) using chelating fluorescent protein chimeras, *J Mol Biol*, 2007, **374**, 411-425.
29. T. H. Evers, M. A. Appelhof, E. W. Meijer and M. Merkx, His-tags as Zn(II) binding motifs in a protein-based fluorescent sensor, *Protein Eng Des Sel*, 2008, **21**, 529-536.
30. Y. Qin, J. G. Miranda, C. I. Stoddard, K. M. Dean, D. F. Galati and A. E. Palmer, Direct comparison of a genetically encoded sensor and small molecule indicator: implications for quantification of cytosolic Zn^{2+}, *ACS Chem Biol*, 2013, **8**, 2366-2371.
31. J. G. Park, Y. Qin, D. F. Galati and A. E. Palmer, New sensors for quantitative measurement of mitochondrial Zn^{2+}, *ACS Chem Biol*, 2012, **7**, 1636-1640.
32. E. A. Bellomo, G. Meur and G. A. Rutter, Glucose regulates free cytosolic Zn^{2+} concentration, Slc39 (ZiP), and metallothionein gene expression in primary pancreatic islet beta-cells, *J Biol Chem*, 2011, **286**, 25778-25789.
33. V. Lanquar, G. Grossmann, J. L. Vinkenborg, M. Merkx, S. Thomine and W. B. Frommer, Dynamic imaging of cytosolic zinc in Arabidopsis roots combining FRET sensors and RootChip technology, *New Phytol*, 2014, **202**, 198-208.
34. P. Chabosseau, E. Tuncay, G. Meur, E. A. Bellomo, A. M. Hessels, S. Hughes, P. R. V. Johnson, M. Bugliani, P. Marchetti, B. Turan, A. R. Lyon, M. Merkx and G. A. Rutter, Mitochondrial and ER-targeted eCALWY probes reveal high levels of free Zn^{2+}, *ACS Chem Biol*, 2014, in press (DOI: 10.1021/cb5004064).
35. H. H. Zeng, E. G. Matveeva, A. K. Stoddard, C. A. Fierke and R. B. Thompson, Long wavelength fluorescence ratiometric zinc biosensor, *J Fluoresc*, 2013, **23**, 375-379.
36. B. J. McCranor, R. A. Bozym, M. I. Vitolo, C. A. Fierke, L. Bambrick, B. M. Polster, G. Fiskum and R. B. Thompson, Quantitative imaging of mitochondrial and cytosolic free zinc levels in an in vitro model of ischemia/reperfusion, *J Bioenerg Biomembr*, 2012, **44**, 253-263.
37. L. Xue, G. Li, C. Yu and H. Jiang, A ratiometric and targetable fluorescent sensor for quantification of mitochondrial zinc ions, *Chemistry*, 2012, **18**, 1050-1054.
38. W. Qiao, M. Mooney, A. J. Bird, D. R. Winge and D. J. Eide, Zinc binding to a regulatory zinc-sensing domain monitored in vivo by using FRET, *Proc Natl Acad Sci U S A*, 2006, **103**, 8674-8679.
39. J. L. Vinkenborg, S. M. van Duijnhoven and M. Merkx, Reengineering of a fluorescent zinc sensor protein yields the first genetically encoded cadmium probe, *Chem Commun (Camb)*, 2011, **47**, 11879-11881.